

Direction-dependent spontaneous emission from near-infrared quantum dots at the angular band edges of a three-dimensional photonic crystal

Jiafang Li, Baohua Jia, Guangyong Zhou, and Min Gu^{a)}

Centre for Micro-Photonics and CUDOS, Faculty of Engineering and Industrial Sciences, Swinburne University of Technology, Hawthorn, Victoria 3122, Australia

(Received 6 August 2007; accepted 21 November 2007; published online 17 December 2007)

Engineering spontaneous emission from light emitters embedded within three-dimensional photonic crystals is of great significance in both fundamental research of quantum optics and applications of microphotonic devices. In this letter, we report on the effective modification of spontaneous emission from near-infrared PbSe quantum dots infiltrated in a three-dimensional woodpile polymeric photonic crystal through adjusting its angle-dependent stop gaps. A significant inhibition effect as well as a pronounced enhancement of the spontaneous emission are observed in the midgap and at the center of the band edge, respectively. The observed phenomenon can be understood from the stretched exponential model on decay dynamics. © 2007 American Institute of Physics. [DOI: 10.1063/1.2824388]

Photonic crystals^{1,2} (PhCs) are periodic structures which have a unique ability to engineer light propagation and emission with their photonic band gap (PBG) properties. Particularly, three-dimensional (3D) PhCs are one of the most promising candidates to form next generation photonic devices.³ A key aspect toward this goal is the development of 3D active PhCs in which light emitters such as quantum dots (QDs) are embedded.²⁻⁴ A large variety of experiments have been reported on the studies of QD emission from opal or inverse opal structures in the visible wavelength range.⁴⁻⁹ Even for partial PBGs of the opal and inverse opal structures, their effects can result in a significant influence on the emission properties of the embedded light emitters, mainly manifested by the changes in photoluminescence (PL) spectra,⁶⁻⁸ the modifications of radiative lifetime,⁹ or the combination of both.⁴ In the near-infrared (NIR) wavelength range, the versatile synthesis and promising optical properties of lead base QDs should provide ideal emitters for 3D PhCs.¹⁰ On the other hand, by using the two-photon polymerization (2PP) method,¹¹⁻¹⁵ high quality 3D woodpile structures with pronounced stop gaps can be fabricated.¹²⁻¹⁷ At the band edges of the stop gaps, the local density of optical states (LDOS) are significantly accumulated.^{4,18} Moreover, pronounced superprism and negative refraction effects, which are highly sensitive to the angle and the frequency of the incident light in the propagation direction inside the crystal, have been observed at the band edges in the telecommunication wavelength range.^{17,19} These PBG and band edge effects provide an interesting physical environment for the investigation of controlling the emission from NIR QDs embedded in a polymer woodpile 3D PhC.

In this letter, we report on the direction-dependent PL dynamics from PbSe QDs infiltrated in a 3D woodpile polymeric PhC at the angular band edges of the PhC. Instead of using different PhC or QD samples, we have achieved different modification effects directly by altering the detection angles of light propagation. Particularly, the inhibition and

enhancement effects of the stop gaps on the spontaneous emission have been observed in the midgap and at the center of the band edge, respectively.

The 3D woodpile PhC in this work was fabricated on a cover glass with Ormocer® (Micro Resist Technology) by using the 2PP method.^{15,17,19,20} To match the stop gaps of the PhCs, we synthesized PbSe QDs with tunable emission in the NIR wavelength range by using the method described by Yu *et al.*²¹ The QDs were infiltrated into the PhC with the method described in Ref. 20 and a QD layer with a thickness of $\sim 10\text{--}20$ nm was deposited onto the surfaces of the PhC rods during the infiltration. In the meantime, a QD film with a thickness of $\sim 0.5\text{--}1$ μm was formed outside the PhC on the cover glass, providing a direct and convenient reference for our studies on QD emission inside the PhC. The dried PbSe QDs on the cover glass were measured to have absorption and emission peaks centered at wavelengths of 1500 and 1580 nm, respectively, with broad PL spectra ranging from 1250 to 1750 nm.²⁰

The stop gaps of the PhC before and after infiltration were measured with a Fourier-transform infrared spectrometer (FTIR) (Thermo Nicolet) in conjunction with an infrared microscope (Continuum). To reduce the averaging effect from the angular distribution of the incident beam in the FTIR on the stop gap measurement, a wedge with a certain angle was used to tilt the sample and a small pinhole was placed in front of the objective to confine the angular distribution to $\sim 5^\circ$ (see inset of Fig. 1).²² The PhC without infiltration was measured to have a stop gap centered at wavelength of 1383 nm. After QD infiltration, the midgap of the PhC was shifted to a longer wavelength at 1400 nm due to the increase in filling ratio and the average refractive index of the structure.²⁰ Angle-dependent stop gaps of the infiltrated sample were measured by varying the tilting angle θ , while the position of the pinhole was kept unchanged (see inset of Fig. 1). As shown in Figs. 2(a)–2(e), the position of the stop gaps of the 3D PhC changes with the angle of incidence θ , especially at larger angles, which is consistent with the prediction of the band gap calculation.¹⁷

^{a)} Author to whom correspondence should be addressed. Electronic mail: mgu@swin.edu.au

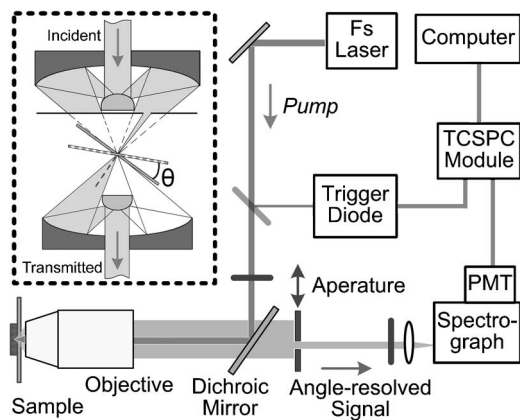


FIG. 1. Sketch for angle-resolved PL decay experiments. Inset: sketch of the reflective objective of FTIR with a pinhole for the angle-confined measurements of stop gaps of PhCs. Angular measurements are realized by changing the tilting angle θ with respect to the axis of the incident beam.

To study the PL decays from QDs inside the PhC at different angles, angle-resolved experiments of the PL decay were conducted by employing the time-correlated single photon counting (TCSPC) technique. As shown in Fig. 1, a high numerical-aperture (NA=1.45) objective with a back aperture diameter of 12 mm was used to focus the beam on the sample and to collect the PL from QDs. To obtain angle-resolved signals, a small aperture (with a diameter of ~ 2 mm) was placed at the back aperture of the objective.⁸ By tuning the lateral position of the small aperture, signals from certain solid angles can be resolved correspondingly. The angle-resolved PL signals were dispersed by a spectrograph (Acton Spectropro 300i) and detected by a fast NIR photomultiplier (Hamamatsu). Single photon counting was carried out using a TCSPC module (PicoHarp 300) con-

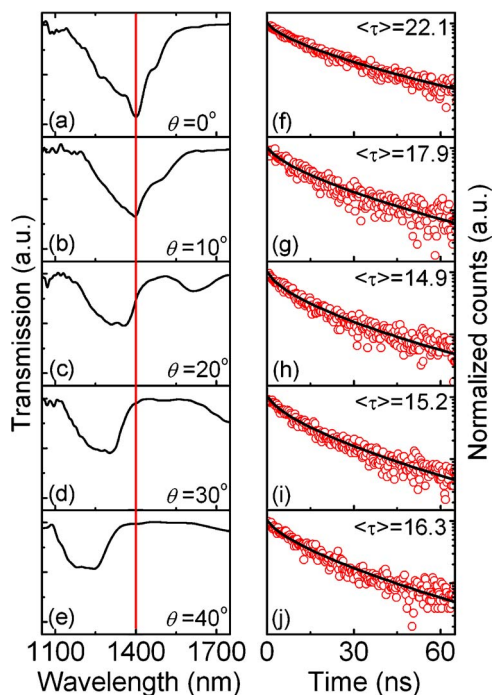


FIG. 2. (Color online) [(a)–(e)] Baseline corrected transmission spectra of the PhC at different angles θ . The vertical solid line indicates the position at wavelength of 1400 nm. [(f)–(j)] Normalized PL decay curves (and $\langle \tau \rangle$) from PbSe QDs inside the PhC at wavelength of 1400 nm at the detection angles corresponding to (a)–(e). Background noise has been subtracted.

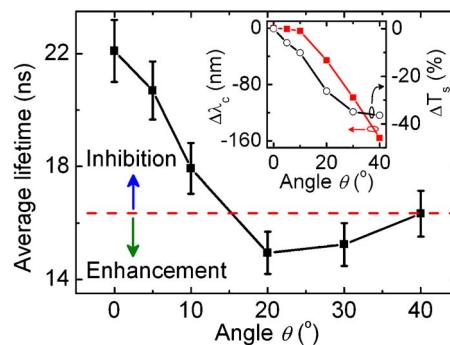


FIG. 3. (Color online) Relationship between the average lifetime $\langle \tau \rangle$ and detection angle θ for PbSe QDs inside the PhC at wavelength of 1400 nm. Inset: the shift of the midgap ($\Delta \lambda_c$, left) and the change in transmission suppression at wavelength of 1400 nm (ΔT_s , right) as a function of θ .

nected to a computer. This system avoided the rotation of the sample and the change of the focus positions, making it suitable for the angle-resolved measurements performed under a constant condition.⁸

The measured PL from PbSe QDs in toluene solution exhibits a single-exponential decay with a lifetime of ~ 480 ns at wavelength of 1580 nm.²⁰ In comparison, the PL decays from dried QDs in air are much faster (only tens of nanoseconds at 1580 nm) and show nonexponential characteristics, mainly due to the energy transfer process among the neighboring PbSe QDs. To get a quantitative evaluate of the radiation properties from the nonexponential PL decays, we fitted the decay curves with the stretched exponential model given by $I(t) = I_0 \exp[-(t/\tau_{1/e})^\beta]$, where $\tau_{1/e}$ is the time constant when the intensity decreases to I_0/e and β ($0 < \beta \leq 1$) is the stretching parameter.^{23,24} The average lifetime $\langle \tau \rangle$ is calculated by $\langle \tau \rangle = (\tau_{1/e}/\beta) \Gamma(1/\beta)$, where Γ represents the gamma function.^{23,24}

Since the PL decays from ensemble QDs are wavelength dependent,²⁰ we focus on the study of the spontaneous emission from QDs at a fixed wavelength of 1400 nm, which is the midgap position at $\theta = 0^\circ$. As shown in Figs. 2(a)–2(e), the relative position of the detection wavelength (1400 nm) with respect to the stop gap is tuned from the midgap through the band edge when θ increases from 0° to 40° . The corresponding PL decays from QDs inside the PhC at wavelength of 1400 nm are plotted in Figs. 2(f)–2(j), where the fitting by the stretching exponential model is also given. It shows clearly that the average lifetime $\langle \tau \rangle$ from QDs inside the PhC changes significantly with θ , while for QDs outside the PhC, little change in $\langle \tau \rangle$ has been observed under the same conditions (not shown), which indicates that the angle-dependent change in $\langle \tau \rangle$ in Figs. 2(f)–2(j) is induced by the stop gaps.

The dependence of $\langle \tau \rangle$ on θ is depicted in Fig. 3, while the dependence of the stop gap and the transmittance at wavelength 1400 nm on θ is illustrated in the inset of Fig. 3, which shows the blueshift of the midgaps ($\Delta \lambda_c$) and the decrease in suppression as θ increases. Since the detection wavelength is far outside the corresponding stop gap at angle 40° [Fig. 2(e)], it is reasonable to use the measured $\langle \tau \rangle$ at this angle ($\langle \tau \rangle_{40}$) as a reference parameter without the influence of the PBG effects. As shown in Fig. 3, $\langle \tau \rangle$ is increased by 35% at $\theta = 0^\circ$, indicating that the QD emission is significantly inhibited at the midgap of the PhC because of the

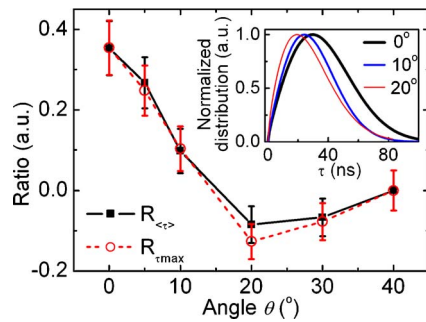


FIG. 4. (Color online) Calculated $R_{\langle\tau\rangle}$ and $R_{\tau_{\max}}$ as a function of θ at wavelength of 1400 nm. Inset: calculated normalized decay time distribution at wavelength of 1400 nm as a function of decay time constant (τ) at different angles θ .

decrease in LDOS. However, at $\theta=20^\circ$, $\langle\tau\rangle$ is decreased by 8.5%, which is a clear reflection of the QD emission enhancement at the center of the band edge of the PhC as a result of the increased LDOS. It should be mentioned that spontaneous emission from infiltrated QDs at wavelength 1625 nm, which is outside the stop gaps of the PhC, does not show such significant angle-dependent decay properties as those at 1400 nm.

The angle-dependent PL decay properties at wavelength 1400 nm can result in the changes in the decay time distributions,^{23,24} which can be calculated with the corresponding parameters $\tau_{1/e}$ and β . The inset of Fig. 4 shows the normalized decay time distribution at different angles θ . It can be seen that the maximum of the decay time distribution τ_{\max} is shifted to shorter times when θ increases from 0° to 20° and that a further increase in θ , however, results in the increase in τ_{\max} , which is similar to the angular dependence of $\langle\tau\rangle$. For comparison, the variations of $\langle\tau\rangle$ and τ_{\max} at different angles at wavelength of 1400 nm are evaluated by the ratios $R_{\langle\tau\rangle} = (\langle\tau\rangle - \langle\tau\rangle_{40}) / \langle\tau\rangle_{40}$ (where $\langle\tau\rangle_{40}$ is the reference average lifetime at $\theta=40^\circ$) and $R_{\tau_{\max}} = (\tau_{\max} - \tau_{\max 40}) / \tau_{\max 40}$ (where $\tau_{\max 40}$ is the maximum decay time distribution at $\theta=40^\circ$), respectively. As shown in Fig. 4, $R_{\langle\tau\rangle}$ and $R_{\tau_{\max}}$ agree well at all angles, which further confirms the angle-dependent PBG effect on the spontaneous emission of QDs inside the PhC.

In conclusion, controlling the dynamics of the spontaneous emission from NIR QDs infiltrated into a 3D PhC has been demonstrated by adjusting the angle-dependent stop gaps of the PhC. An inhibition by up to 35% and an enhance-

ment by up to 8.5% of the spontaneous emission have been observed in the mid-gap and at the center of the band edge, respectively. This work provides an effective way to tune the spontaneous emission from QDs by engineering the PBG effects in a given 3D PhC, especially in the important telecommunication wavelength range.

This work was produced with the assistance of the Australian Research Council (ARC) under the ARC Centres of Excellence program. CUDOS (the Centre for Ultrahigh-bandwidth Devices for Optical Systems) is an ARC Centre of Excellence.

- ¹E. Yablonovitch, Phys. Rev. Lett. **58**, 2059 (1987).
- ²S. John, Phys. Rev. Lett. **58**, 2486 (1987).
- ³S. Noda, K. Tomoda, N. Yamamoto, and A. Chutinan, Science **289**, 604 (2000).
- ⁴P. Lodahl, A. F. Van Driel, I. S. Nikolaev, A. Irman, K. Overgaag, D. Vanmaekelbergh, and W. L. Vos, Nature (London) **430**, 654 (2004).
- ⁵Yu. A. Vlasov, K. Luterova, I. Pelant, B. Hönerlage, and V. N. Astratov, Appl. Phys. Lett. **71**, 1616 (1997).
- ⁶A. Blanco, C. Lopez, R. Mayoral, H. Miguez, F. Meseguer, A. Mifsud, and J. Herrero, Appl. Phys. Lett. **73**, 1781 (1998).
- ⁷Y. Lin, J. Zhang, E. H. Sargent, and E. Kumacheva, Appl. Phys. Lett. **81**, 3134 (2002).
- ⁸M. Barth, A. Gruber, and F. Cichos, Phys. Rev. B **72**, 085129 (2005).
- ⁹J.-Y. Zhang, X.-Y. Wang, M. Xiao, and Y.-H. Ye, Opt. Lett. **28**, 1430 (2003).
- ¹⁰R. D. Schaller, M. A. Petruska, and V. I. Klimov, J. Phys. Chem. B **107**, 13765 (2003).
- ¹¹S. Kawata, H.-B. Sun, T. Tanaka, and K. Takada, Nature (London) **412**, 697 (2001).
- ¹²M. Straub and M. Gu, Opt. Lett. **27**, 1824 (2002).
- ¹³L. H. Nguyen, M. Straub, and M. Gu, Adv. Funct. Mater. **15**, 209 (2005).
- ¹⁴S. Wu, J. Serbin, and M. Gu, J. Photochem. Photobiol., A **181**, 1 (2006).
- ¹⁵B. Jia, J. Li, and M. Gu, Aust. J. Chem. **60**, 484 (2007).
- ¹⁶M. Deubel, G. von Freymann, M. Wegener, S. Pereira, K. Busch, and C. M. Soukoulis, Nat. Mater. **3**, 444 (2004).
- ¹⁷J. Serbin and M. Gu, Adv. Mater. (Weinheim, Ger.) **18**, 221 (2006).
- ¹⁸K. Busch and S. John, Phys. Rev. B **58**, 3896 (1998).
- ¹⁹J. Serbin and M. Gu, Opt. Express **14**, 3563 (2006).
- ²⁰J. Li, B. Jia, G. Zhou, J. Serbin, C. Bullen, and M. Gu, Adv. Mater. (Weinheim, Ger.) **19**, 3276 (2007).
- ²¹W. W. Yu, J. C. Falkner, B. S. Shih, and V. L. Colvin, Chem. Mater. **16**, 3318 (2004).
- ²²J. Li, B. Jia, G. Zhou, and M. Gu, Opt. Express **14**, 10740 (2006).
- ²³G. Schlegel, J. Bohnenberger, I. Potapova, and A. Mews, Phys. Rev. Lett. **88**, 137401 (2002).
- ²⁴The decay time distribution function is given by $G(\tau) = \tau\rho(\tau)$, where $\rho(\tau)$ is defined by $e^{-(t/\tau_{1/e})^\beta} = \int_0^\infty e^{-t\tau} \rho(\tau) d\tau$ with $\rho(\tau) = -(\tau_{1/e}/\pi\tau^2) \times \sum_0^\infty [(-1)^k/k!] \sin(\pi\beta k) \Gamma(\beta k + 1) (\tau/\tau_{1/e})^{\beta k + 1}$. C. P. Lindsey and G. P. Patterson, J. Chem. Phys. **73**, 3384 (1980).